A new combined multicompartmental model for apolipoprotein B-100 and triglyceride metabolism in VLDL subfractions

Martin Adiels,* Chris Packard,† Muriel J. Caslake,† Philip Stewart,† Aino Soro,§ Jukka Westerbacka,§ Bernt Wennberg,* Sven-Olof Olofsson, Marja-Riitta Taskinen,§ and Jan Borén[1],****

Mathematical Sciences,* Chalmers University of Technology, 412 96 Göteborg, Sweden; Department of Pathological Biochemistry,† Glasgow Royal Infirmary, G31 2ER Glasgow, United Kingdom; Division of Cardiology,§ Helsinki University Hospital, Biomedicum, 00029 Helsinki, Finland; and Wallenberg Laboratory,** Göteborg University, 413 25 Göteborg, Sweden

Abstract **The use of stable isotopes in conjunction with compartmental modeling analysis has greatly facilitated studies of the metabolism of the apolipoprotein B (apoB)-containing lipoproteins in humans. The aim of this study was to develop a multicompartment model that allows us to simultaneously determine the kinetics of apoB and triglyceride (TG) in $VLDL_1$ and $VLDL_2$ after a bolus injection of [$^2H_3$]leucine and [$^2H_5$]glycerol and to follow the catabolism and transfer of the lipoprotein particles. Here, we describe the model and present the results of its application in a fasting steady-state situation in 17 subjects with lipid values representative of a Western population. Analysis of the correlations showed that plasma TG was determined by the $VLDL_1$ and $VLDL_2$ apoB and TG fractional catabolic rate. Furthermore, the model showed a linear correlation between $VLDL_1$ TG and apoB production. A novel observation was that VLDL TG entered the circulation within 21 min after its synthesis, whereas VLDL apoB entered the circulation after 33 min. These observations are consistent with a sequential assembly model of VLDL and suggest that the TG is added to a primordial apoB-containing particle in the liver.**—Adiels, M., C. Packard, M. J. Caslake, P. Stewart, A. Soro, J. Westerbacka, B. Wennberg, S-O. Olofsson, M-R. Taskinen, and J. Borén. **A new combined multicompartmental model for apolipoprotein B-100 and triglyceride metabolism in VLDL subfractions. *J. Lipid Res.* 2005.** 46: **58–67.**

Supplementary key words very low density lipoprotein • kinetics • stable isotope • assembly

Regulation of the metabolism of VLDL subfractions has been an area of active interest that received fresh impetus from the introduction of stable isotope-based techniques in the late 1980s (1, 2). The use of tracer models has generated direct information on lipoprotein synthetic rates, which previously could only be inferred from the turnover of radiolabeled lipoproteins. One common approach is to inject a bolus of radioactive tracer, such as [^{3}H,^{14}C]glycerol, and determine the subsequent monoexponential slope of the decline in plasma VLDL-specific radioactivity. A disadvantage of this approach is that it can underestimate the true VLDL turnover rate because it does not account for recycling of the injected bolus of tracer (3). Multicompartmental modeling improves the accuracy by attempting to account for tracer recycling (3–8). Such studies have revealed that $VLDL_1$ apolipoprotein B-100 (apoB-100) production and $VLDL_2$ apoB-100 production are independently regulated (9–11), indicating that regulatory steps in the assembly of VLDL govern the lipid content of the secreted particles. However, it is still unclear how the liver regulates the triglyceride (TG) content of VLDL particles to produce large $VLDL_1$ or small $VLDL_2$. VLDL assembly is thought to involve at least two steps in which nascent VLDL particles are formed and then TG is added, resulting in larger particles (12, 13).

Several studies have analyzed VLDL TG turnover kinetics using stable isotopically labeled glycerol or palmitate tracers and mathematical modeling. However, VLDL subclasses were not analyzed in those studies, and VLDL apoB was not included in the models (3, 14, 15). To enhance our understanding of the pathways leading to $VLDL_1$ and $VLDL_2$ and of the metabolic fate of these particles, we developed for the first time a multicompartmental mathematical model that allows the kinetics of TG and apoB-100 in $VLDL_1$ and $VLDL_2$ to be simultaneously assessed after a bolus injection of glycerol and leucine. Here, we describe

Manuscript received 17 March 2004 and in revised form 26 July 2004 and in re-revised form 30 September 2004.

Published, JLR Papers in Press, October 16, 2004.
DOI 10.1194/jlr.M400108-JLR200

[1] To whom correspondence should be addressed.
e-mail: jan.boren@wlab.gu.se

the model and present the results of its application in 17 subjects with lipid values representative of a Western population.

METHODS

Subjects and materials

Seventeen healthy subjects were recruited for this study. The purpose, nature, and potential risks of the study were explained to all subjects before their written consent was obtained. The study protocols were approved by the Ethical Committee of the Helsinki University Central Hospital. All materials were from Sigma Chemical Co. (Poole, Dorset, UK) unless otherwise stated.

ApoB and TG turnover protocol

All subjects were admitted at 7:30 AM to the metabolic ward of the Helsinki University Central Hospital after a 12 h overnight fast. An indwelling cannula was inserted into an antecubital vein for infusions. A second cannula was inserted retrogradely into a heated hand vein to obtain arterialized venous blood for sampling. A saline infusion was started. Thirty minutes later, leucine (5,5,5-D3), 7 mg/kg body weight, and glycerol (1,1,2,3,3-D5), 500 mg (Isotec, Miamisburg, OH), were injected as a bolus. For the measurement of free [$^2H_3$]leucine concentrations in plasma, blood samples were taken before the tracer injection and at 2, 4, 6, 8, 10, 12, 15, 20, 30, and 45 min and 1, 2, 3, 4, 6, and 8 h. For the measurement of [$^2H_3$]leucine and [$^2H_5$]glycerol in $VLDL_1$ and $VLDL_2$, blood samples were taken before the injection of tracers and at 15, 30, 45, 60, 75, 90, 120, and 150 min and 3, 4, 5, 6, 7, and 8 h. The particle composition and apoB mass of the $VLDL_1$ and $VLDL_2$ fractions were determined 30 min before and 0, 4, and 8 h after the injection. The subjects continued to fast until 5 PM, when the last blood sample was taken.

Isolation of lipoproteins

$VLDL_1$ and $VLDL_2$ were isolated from 8.4 ml of plasma as described (16). The apoB and TG pool sizes were analyzed from samples obtained at 0, 4, and 8 h and prepared as described (16). Pool sizes for apoB and TG were calculated as the product of plasma volume (4.5% of body weight) and the plasma concentration of apoB and TG in $VLDL_1$ and $VLDL_2$. The leucine content of the apoB pool was calculated from the apoB amino acid residue composition. The glycerol content was calculated from the TG concentration using a molar weight of 885 g/mol for TG and 92 g/mol for glycerol and assuming that 1 mol of TG equals 1 mol of glycerol.

Biochemical analyses

TG and cholesterol concentrations in total plasma and in all lipoprotein fractions were determined by automated enzymatic methods (Cobas Mira analyzer; Hoffman-La Roche, Basel, Switzerland). ApoB was analyzed in the plasma lipoprotein fractions as described (17). Serum glucose, insulin, free fatty acids, and alanine transaminase were analyzed as described (18). Protein concentrations in lipoprotein fractions were measured by the method of Kashyap, Hynd, and Robinson (19).

Determination of leucine enrichment in apoB

The samples were precipitated with isopropanol, delipidated with ethanol-diethyl ether, dried, and hydrolyzed with 6 M HCl at 110°C for 22–24 h (16). The samples were then prepared for analysis of leucine enrichment (20), and the [$^2H_3$]leucine enrichments in protein hydrolysates and plasma amino acids were performed as described (21). Enrichments were determined by GC-MS with a quadrupole GC-MS instrument (MD 800; Fisons, Manchester, UK).

Determination of glycerol enrichment in TG

The samples were precipitated with isopropanol and delipidated twice with ethanol-diethyl ether as described (20). The supernatants were combined, and the volume was increased to 20 ml with isopropanol. To remove phospholipids, 2 g of activated zeolite (product no. 96096; Fluka Biochemika, Buchs, Switzerland) was added to each tube and mixed for 20 min. After centrifugation, the supernatants were evaporated under N_2 at 80°C. Isopropanol (1 ml) was added to each tube, transferred into a 1.5 ml vial, and dried on a heating block at 80°C. The glycerol samples were stored at −80°C. The amount of diacylglycerol and monoacylglycerols not extracted in the supernatant was not determined. This has been reported to be a minor contaminant, accounting for 2–10% of the total plasma TG (22). Immediately before analysis, the glycerol extracts were saponified with 250 μl of 2% KOH in ethanol, incubated at 60°C for 2 h, and dried under N_2 at 70°C for 2 h.

In three subjects, glycerol was isolated as described by Patterson et al. (23). Briefly, plasma proteins were precipitated with ice-cold acetone, equal volumes of hexane and water were added to the supernatant, and the upper phase (hexane) was dried in a centrifugal evaporator.

Glycerol was derivatized to its 1,2,3-triacetate ester by adding equal volumes of pyridine and acetic anhydride (24). Enrichments were determined with a quadrupole GC-MS instrument (Trio-1000; Fisons) under electron ionization conditions within 24 h after saponification. Samples (1–3 μl) were injected automatically into a 30 m × 0.25 mm (inner diameter) × 0.25 μm DB5MS capillary column fitted with a 2 m plain silica guard column (J&W, Folsom, CA), which was run isothermally at 195°C, using a split ratio of 1:50, helium as the carrier gas, and a head pressure of 70 kPa (10 pounds per square inch). The glycerol derivative eluted at ~3.5 min. Under these conditions, the derivative fragments between carbons 1 and 2 or 2 and 3 of the glycerol backbone resulted in the formation of two symmetrical fragments of *m/z* 145 and two symmetrical fragments of *m/z* 73 for the unlabeled derivative (24).

The penta-deuterated derivative formed a tri-deuterated fragment at *m/z* 148 and a bi-deuterated fragment at *m/z* 75. Monitoring the larger fragment (*m/z* 148) allowed measurements to be made against a very low natural background, resulting in greater sensitivity than monitoring the smaller ion fragment. Ion mass fragments at *m/z* 147 and 148 were monitored in the selective ion recording mode. Ion peaks areas were integrated and quantified in arbitrary units with the LabBase GC-MS data management system (Fisons).

To calculate isotope enrichments, the average value of the *m/z* 147:145 ratio was determined in the baseline sample. This value was multiplied by the *m/z* 148:147 ratio, and the resulting *m/z* 148:145 values were expressed as molar percentage excess (mpe) by the following formula:

$$\text{mpe} = [(IR_t - IR_b) / (1 + (IR_t - IR_b))] \times 100$$

where IR_t is the *m/z* 148:145 peak area ratio for the enriched sample at time t and IR_b is the equivalent ratio for the baseline (0 h) sample.

Monitoring of the m+3 and m+2 peaks permitted greater loading of the GC-MS apparatus and enhanced our ability to detect low enrichments with good precision, as we do for leucine enrichment in apoB (21). Standards with enrichments of 0.00–1.00 mpe were included at the beginning and end of each batch of samples and used to correct the calculated mpe values with

the calculated recovery rate of the standards. Care was taken to ensure similar total ion counts in the standards and all samples.

In three subjects, the *m/z* 148, 147, 146, and 145 peaks was measured to compare the glycerol enrichment by assessing the d5-glycerol tracer as an entire moiety in GC-MS analysis and by the technique described above.

Model development

The measurements of enrichment of free leucine in plasma, $VLDL_1$, and $VLDL_2$, enrichment of glycerol in $VLDL_1$ and $VLDL_2$, the pool sizes of leucine and glycerol (i.e., derived from apoB and TG) in $VLDL_1$ and $VLDL_2$, and the known injected amounts of labeled leucine and glycerol were used to determine kinetic parameters using the modeling software SAAMII (SAAM Institute, Seattle, WA) and Matlab. By simultaneously modeling apoB and TG kinetics, it was possible to determine the TG/apoB ratio of newly produced $VLDL_1$ and $VLDL_2$ particles and to follow in detail the transfer and removal of lipids.

The data were analyzed with two linear compartmental models. The proposed apoB/TG model can be envisioned as a two layer model, connected at certain points, and is based on the apoB model originally described by Packard et al. (25), which has been used in several studies (9, 10, 25–29). Basically, the model consists of four parts: plasma leucine, plasma glycerol, the assembly of lipoprotein, and lipoprotein plasma kinetics.

Modeling of plasma leucine

Free plasma leucine was modeled as a four-compartment catenary system (**Fig. 1**). Compartment 1 is the plasma compartment, where the leucine is injected. Compartments 3 and 4 are protein pools, which give a slow release of leucine. Compartment 2 is an intracellular compartment from which the leucine is transferred into the liver's apoB synthetic machinery. The transfer coefficients between compartments 1 and 2 are equal, giving equilibrium. To further decrease the number of unknowns, $k_{3,4}$ is set at 0.1 $k_{4,3}$ (i.e., the transfer from compartment 4 to 3 is one-tenth of the transfer from compartment 3 to 4) (26). Other approaches such as a forcing function, determined from measurements, could also be used.

Modeling of plasma glycerol

TG assembly was modeled with a modified variant of a model described by Zech et al. (4). The plasma compartment (i.e., compartment 13) is connected to an extrahepatic pool (compartment 12). The fractional transfer coefficients are fixed by the population means as described by Zech et al. (4): $k_{12,13} = 12$, $k_{13,12} = 5$, and $k_{0,13} = 19$ [h^{-1}] (Fig. 1). This restriction could be relaxed by measurements of enrichment of free glycerol in plasma and to either choose parameters to fit the data or use a forcing function determined by the data. To justify the approach of population means, we have made measurements of plasma glycerol and compared the kinetic parameters determined by the two models.

Modeling of lipoprotein assembly

The TG conversion (compartment 14) has influx from compartment 13, and a slow path for conversion is implemented as compartment 21 interchanging materials with compartment 14. Compared with the model by Zech et al. (4), the slow pathway was modeled by compartment 21 instead of a compartment with influx from compartment 13 and outfluxes into compartments 5 and 8. The reason for choosing the current model is the reduced complexity of the model. Both models allow for a slow production pathway (most noticeable after 8 h), but the current implementation does not allow for a small amount of material to rapidly pass through the slow pathway.

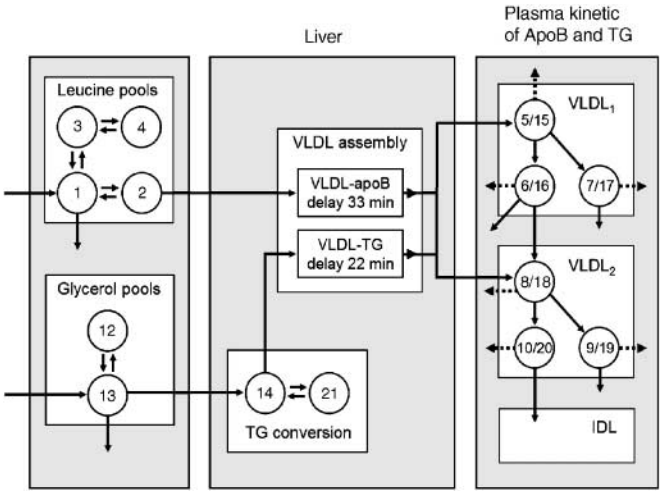

Fig. 1. Schematic model of the two-layer compartmental model. The model includes separate modules for leucine and glycerol. The assembly of lipoprotein is modeled by separate delays for apolipoprotein B-100 (apoB) and triglyceride (TG). The plasma kinetics is modeled by a four-compartment hydrolysis chain, in which the apoB and TG kinetics are coupled at the transfer between compartments. The free leucine plasma kinetics is modeled by two pools (3 and 4) and a plasma compartment (1), which interchange materials with an intracellular compartment (2). Compartment 2 feeds the apoB synthetic machinery. For glycerol, the plasma compartment (13) is connected to a pooling compartment (12) and feeds TG synthesis, which consists of a fast pathway (14) and a slow pathway (21). ApoB synthesis and the synthesis of lipoproteins are modeled by two delays initially set to 0.5 h (leucine) and 0.3 h (glycerol). The plasma kinetics of apoB and TG is modeled by a four-compartment hydrolysis chain, consisting of compartments 5, 6, 8, and 10 for apoB. Each apoB compartment, *i*, has an associated TG compartment, *i+10*, denoted as 15, 16, and so forth. Compartments 5/15 and 6/16 are associated with $VLDL_1$, together with a slowly decaying compartment 7/17. Compartments 8/18 and 10/20 together with the slowly decaying compartment 9/19 form the $VLDL_2$ module. Lipolysis of TG is modeled to take place in the transfer between two compartments. When a particle is being removed from the source, *i*, compartment, only a fraction, $f_{j,i}$, of the TG ends up in the destination compartment, *j*. The rest, $1 - f_{j,i}$, is removed by the hydrolysis. The fractional transfer coefficients for the TG compartments are defined as follows:

$$k_{j+10,\,i+10} = f_{j,i}k_{j,i},\quad k_{0,i+10} = k_{0,i} + \sum_{j=5}^{10}(1 - f_{j,i})k_{j,i}$$

Hence, direct removal from TG compartments consists of both the removal of whole particles (solid arrows) and the removal of TG (dashed arrows).

In theory, information regarding the extent of tracer recycling in the liver through compartment 21 could be obtained by following VLDL kinetics over a prolonged period (e.g., 24 h). In the latter stages, the input of tracer into VLDL would be dominated by internally recycled material via compartment 21 (i.e., material stored in compartment 21 and released back to compartment 14). Over the 8 h of the current experiments, there was limited ability to define this "tail" of the VLDL curve with precision (4, 30).

The synthesis of apoB and lipoproteins was modeled by two delays, a seven-compartment delay initially set to 0.5 h for apoB and a five-compartment delay initially set to 0.3 h for TG (Fig. 1).

Modeling of $VLDL_1$ and $VLDL_2$ kinetics

In the underlying apoB model (Fig. 1), a particle is thought of as moving downward (i.e., to a higher density lipoprotein) as it moves from one compartment to another. The TG/apoB decreases as the density increases. Hence, for an apoB particle to move downward in the model, its carrier lipoprotein must lose TG.

Focusing on the apoB model (Fig. 1), the hydrolysis chain is modeled by a four-compartment chain (compartments 5, 6, 8, and 10) and two slowly decaying compartments (7 and 9). $VLDL_1$ consists of compartments 5, 6, and 7, and $VLDL_2$ consists of compartments 8, 10, and 9. Direct removal of apoB (and hence whole particles) is allowed from compartments 6, 7, 9, and 10. Particles in compartment 10 can be removed both by direct removal and by transfer to intermediate density lipoprotein (IDL). However, it is not possible to separate these without sampling IDL apoB enrichments and measuring the pool size.

VLDL TG kinetics is often modeled by a single compartment (i.e., having monoexponential decay), but our goal was to use the same model used for apoB. This made it possible to extract quantities such as the TG/apoB ratio of newly produced particles. Using different models for apoB and TG would have made it impossible to compare the transfer rates of apoB and TG.

Mathematically, a compartment is defined as an amount of material with homogeneous kinetics. Therefore, all particles in an apoB compartment should be thought of as having similar kinetics, and their average TG/apoB ratio is the ratio of the pools. However, there are variations of composition and size within VLDL subfractions, and the true distribution of lipoprotein particles is continuous. Thus, a small $VLDL_1$ particle might be smaller than a large $VLDL_2$ particle, and consequently the TG/apoB ratio of some $VLDL_1$ particles may be lower than that of some $VLDL_2$.

The TG model shares the structure of the apoB model, in which each apoB compartment (5, 6, etc.) has a corresponding TG compartment number (15, 16, etc.).

There are several ways to connect the TG model to the apoB model. Here, we present an intuitive approach in which the TG is removed in the transition between two compartments. We denote the TG/apoB ratio in a compartment by A_i, so the TG mass in a compartment is $Q_{(i+10)} = A_i \times Q_i$. Furthermore, the fraction of the TG that is removed during the transition is denoted $(1 - f_{j,i})$. More precisely, the TG/apoB ratio of a particle that leaves compartment i is A_i, the amount of TG per apoB that is removed from that particle is $(1 - f_{j,i})A_i$, and the TG/apoB ratio of the particle when it enters the destination compartment, j, is $f_{j,i} \times A_i$. Therefore, the fractional transfer coefficients for the TG compartments are defined as follows:

$$k_{j+10,i+10} = f_{j,i}k_{j,i}, \quad k_{0,i+10} = k_{0,i} + \sum_{j=5}^{10}(1 - f_{j,i})k_{j,i}$$

where $i, j, = 5, \ldots 10$.

The steady-state assumption posits that A_5 equals the ratio of the TG and apoB fluxes into compartments 15 and 5. Furthermore $A_6 = A_5 \times f_{6,5}$, $A_7 = A_5 \times f_{7,5}$, $A_8 = A_6 \times f_{8,6}$, etc. $VLDL_2$ particles synthesized in the liver and derived from $VLDL_1$ should have the same TG/apoB ratio. This is determined by defining the fraction of TG going into $VLDL_1$, d_{15}, as follows:

$$d_{15} = \frac{d_5}{d_5 + f_{8,6}f_{6,5}(1 - d_5)}$$

where d_5 is the fraction of apoB going into $VLDL_1$. The unknown parameters in the model are the apoB transfer coefficients and the $f_{j,I}$ values.

An alternative model that gives comparable results (production and catabolic rates) has been described in detail by Adiels (31).

In the model, direct removals from compartments 6 and 16 were initially set to zero and were allowed to be greater than zero only if no satisfactory fit could be achieved. The value for direct removal was then defined as the lowest value to produce a goodness of fit within 1% of maximal goodness of fit (achieved with no limit of direct removal).

The parameters determined in the model are the parameters in the apoB model; that is, the fractional transfer coefficients between compartments 1–10, with the constraints $k_{3,4} = 0.1\ k_{4,3}$ and $k_{1,2} = k_{2,1}$ as described above, $k_{8,6} = k_{6,5}$, $k_{0,10} = k_{10,8}$ and the delay time as well as the fractions of apoB going to $VLDL_1$ and $VLDL_2$ (d_5 and $d_8 = 1 - d_5$). For the TG, the fractional transfer coefficients corresponding to the liver kinetics ($k_{14,12}$, $k_{14,21}$, and $k_{21,14}$) were determined as well as the transfer from compartment 14 to the delay compartment, the delay time and the fractions of TG being transferred between compartments (i.e., the $f_{i,j}$ values).

Statistical analysis

Bivariate correlations were determined by linear regression. Before regression was applied, the data were transformed to achieve a linear relationship. Statistical analysis was performed using Microsoft™ Excel.

Calculated parameters

From the calculated solution to the model, we calculated the fractional catabolic rate (FCR; i.e., total fractional loss of apoB/TG from $VLDL_1$ and $VLDL_2$), the fractional direct catabolic rate (FDCR; i.e., fractional loss of apoB/TG from $VLDL_1$ as a result of direct catabolism and hydrolyzation), and the fractional transfer rate (FTR; i.e., fractional transfer of apoB/TG from $VLDL_1$ to $VLDL_2$). The mean residence time for a particle in $VLDL_1$ and $VLDL_2$ was calculated as the reciprocal of the corresponding FCR, and the production of apoB and TG was calculated as mg/day/kg body weight. The model does not allow us to discriminate the transfer of $VLDL_2$ to IDL from direct removal, because IDL is not included in the model.

List of equations

The flow of material from a compartment, k, to another compartment, l, or the environment, $l = 0$, is defined as follows:

$$\mathrm{FTR}^{\mathrm{apoB}} = \frac{FLUX(8,6)}{Q_5 + Q_6 + Q_7}$$

$$\mathrm{FCR}^{\mathrm{apoB}}_{\mathrm{VLDL}_1} = \frac{FLUX(0,6) + FLUX(8,6) + FLUX(0,7)}{Q_5 + Q_6 + Q_7}$$

$$\mathrm{FDCR}^{\mathrm{apoB}}_{\mathrm{VLDL}_1} = \frac{FLUX(0,6) + FLUX(0,7)}{Q_5 + Q_6 + Q_7}$$

$$\mathrm{FCR}^{\mathrm{apoB}}_{\mathrm{VLDL}_2} = \frac{FLUX(0,9) + FLUX(0,10)}{Q_8 + Q_9 + Q_{10}}$$

$$\mathrm{FTR}^{\mathrm{TG}} = \frac{FLUX(18,16)}{Q_{15} + Q_{16} + Q_{17}}$$

$$\mathrm{FCR}^{\mathrm{TG}}_{\mathrm{VLDL}_1} = \frac{FLUX(0,15) + FLUX(0,16) + FLUX(18,16) + FLUX(0,17)}{Q_{15} + Q_{16} + Q_{17}}$$

$$\mathrm{FDCR}^{\mathrm{TG}}_{\mathrm{VLDL}_1} = \frac{FLUX(0,15) + FLUX(0,16) + FLUX(0,17)}{Q_{15} + Q_{16} + Q_{17}}$$

$$\mathrm{FCR}^{\mathrm{apoB}}_{\mathrm{VLDL}_2} = \frac{FLUX(0,18) + FLUX(0,19) + FLUX(0,20)}{Q_{18} + Q_{19} + Q_{20}}$$

TABLE 1. Baseline characteristics

Characteristic	Mean ± SD	Range
Age (years)	49 ± 9	25–59
Weight (kg)	82.2 ± 8.7	69.8–97.5
Body mass index (kg/m^2)	26.4 ± 2.4	22.4–30.1
Alanine transaminase (IU)	26 ± 7	14–39
Insulin (mU/l)	5.9 ± 2.1	2–10
Plasma glucose (mg/dl)	107 ± 10	90.5–130
TG (mmol/l)	1.54 ± 0.46	0.99–2.59
Cholesterol (mmol/l)	5.2 ± 1.0	4.0–7.5
HDL (mmol/l)	1.34 ± 0.23	0.93–1.68
FFA (μmol/l)	520 ± 98	319–648
apoB (mg/dl)	104 ± 24	66–140

apoB, apolipoprotein B-100; TG, triglyceride.

RESULTS

Catabolic and transfer rates of VLDL subclasses

The 17 subjects (all men) had a mean age of 49 ± 9 years, a mean body mass index of 26.4 ± 2.4 kg/m^2, and lipid values representative of a Western population (**Table 1**). The multicompartmental model (Fig. 1) was developed and used to determine the kinetics of apoB and TG in $VLDL_1$ and $VLDL_2$ in all subjects, and the catabolic and transfer rates for both $VLDL_1$ and $VLDL_2$ were calculated (Table 1). Typical enrichment curves and fit to the model are shown in **Fig. 2**.

TG production was 107–347 mg/day/kg in $VLDL_1$ and 9.5–51.8 mg/day/kg in $VLDL_2$ (**Table 2**). These values correspond to 8–30 g/day and 0.7–4.6 g/day, respectively. TG was removed from $VLDL_1$ by three pathways: particles transferred from $VLDL_1$ to $VLDL_2$ (characterized by the $VLDL_1$ FTR), particles removed by direct catabolism (i.e., $VLDL_1$ particle uptake by cells), and TG removal by hydrolysis. The latter two are combined into the FDCR.

Parameter-free analysis

Analysis of the enrichment curves (Fig. 2) shows that the enrichment rapidly increases, which indicates that the influx is much greater than the outflux. In the peak area, either the influx starts to decrease or the outflux balances the influx. In the rapid decay interval of the curve, the outflux dominates the influx. After the peak of $VLDL_1$, labeled material enters $VLDL_2$ both directly from the liver and from $VLDL_1$.

In the initial part of the enrichment curve, all enriched material that has been secreted is within the pool. Let E be the total amount of enriched material secreted and a the fraction that is secreted as $VLDL_1$. Hence, the fraction secreted as $VLDL_2$ is $(1 - a)$. We denote the $VLDL_1$ pool P_1 and the $VLDL_2$ pool P_2 and the enrichment of $VLDL_1$ E_1 and the enrichment of $VLDL_2$ E_2. Thus, $E_1 = E \times a/P_1$ and $E_2 = E \times (1 - a) \times P_2$, and $E_1/E_2 = P_2 \times a/(P_1 \times (1 - a))$ or $a = 1 - P_2/(P_2 + P_1 \times E_1/E_2)$. By approximating the initial slope by a straight line, we estimated E_1 and E_2, and using the pool size measurements averaged over the three time points, we calculated the fraction of particles and the fraction of TG going into $VLDL_1$ and $VLDL_2$ within a few percentage points (data not shown).

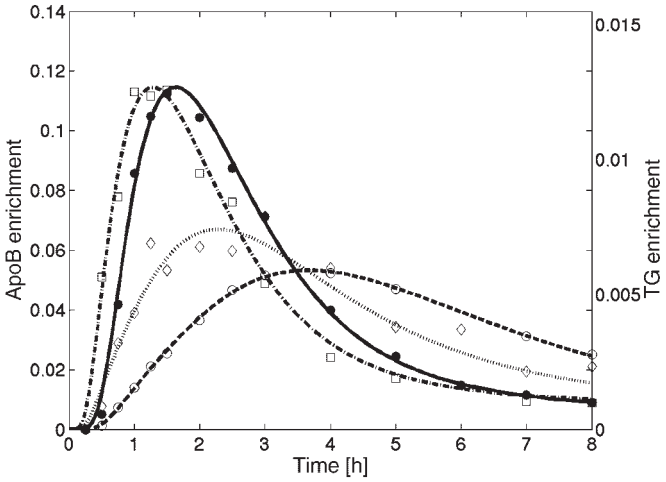

Fig. 2. Typical TG and apoB enrichment curves (subject 7). TG $VLDL_1$ (open squares, dash-dot line) and $VLDL_2$ (open diamonds, dotted line) are scaled so the TG $VLDL_1$ matches the apoB $VLDL_1$ (closed circles, solid line). ApoB $VLDL_2$ is shown as well (open circles, dashed line). The $VLDL_1$ curves are similar in shape, but the $VLDL_2$ curves show differences in the initial slope and in clearance. The difference in delay times is clearly shown.

TG kinetics approximated by apoB kinetics

To further predict the TG model, we have used the calculated apoB kinetics to approximate the TG FDCR. The FDCR for TG is composed of direct removal of whole particles and removal of lipids by hydrolysis. The amount of TG removed as a result of direct removal of particles can be estimated by the FDCR(apoB) times the average TG/apoB ratio. The loss of TG to lipolysis is the FTR(apoB) times the difference in size of a $VLDL_1$ particle and a $VLDL_2$ particle. There is also an unknown term of the amount of TG that has to be removed to form an average size $VLDL_1$ particle. Hence, a low estimate of the TG FDCR is as follows:

$$\mathrm{FDCR}_{TG} = \frac{\mathrm{FDTR}_{apoB} \times R_1 + \mathrm{FTR}_{apoB} \times (R_1 - R_{1/2})}{R_1}$$

Using $R_{1/2} = (R_1 + R_2)/2$, we get estimates of FDCR that are on average 30% lower than the model-derived FDCR. Using average values from the subjects in this study (Table 2), we calculated the FDCR to be 8.2, which should be compared with the average of the model FDCRs, which was 11.5.

Impact of population means for plasma glycerol

In three subjects, the plasma glycerol enrichment was measured and included in the model and the fractional transfer coefficients between and from compartments 13 and 12 were allowed to vary. These subjects were also modeled with the usual model. Even if the individual transfer coefficients varied between the two models, the derived kinetic parameters, such as production and the FCR, were within 15%, suggesting that the use of fixed transfer coefficients gives reasonable results for normal subjects.

TABLE 2. Plasma concentrations of VLDL, TG/apoB ratios, and calculated parameters: transfer rate, catabolic rate, and production rate

	Measured		Calculated	
Variable	Mean ± SD	Range	Mean ± SD	Range
$VLDL_1$ TG pool (mg/kg bw)	19.2 ± 11.4	4.7–47	18.3 ± 10.7	4.2–41
$VLDL_2$ TG pool (mg/kg bw)	7.2 ± 3.6	2.20–14.3	7.1 ± 3.6	1.70–14.4
$VLDL_1$ apoB pool (mg/kg bw)	0.75 ± 0.52	0.16–2.11	0.70 ± 0.46	0.15–1.74
$VLDL_2$ apoB pool (mg/kg bw)	1.23 ± 0.65	0.29–2.64	1.22 ± 0.65	0.27–2.69
$VLDL_1$ TG/apoB pool (mg/mg)	27.2 ± 3.6	22.0–33.6	27.2 ± 5.14	17.3–37.7
$VLDL_2$ TG/apoB pool (mg/mg)	6.08 ± 1.00	4.27–7.76	5.94 ± 0.94	4.27–7.84
$VLDL_1$ TG/apoB production (mg/mg)			33.4 ± 8.4	19.7–49.4
$VLDL_2$ TG/apoB production (mg/mg)			14.3 ± 4.0	6.9–21.3
$VLDL_1$ TG FCR (pools/day)			15.2 ± 8.9	5.7–35.5
$VLDL_1$ TG FDCR (pools/day)			11.5 ± 8.6	4.2–33.0
$VLDL_1$ TG FTR (pools/day)			3.73 ± 1.84	1.53–8.62
$VLDL_2$ TG FCR (pools/day)			14.0 ± 7.8	5.8–39.4
VLDL TG FCR (pools/day)			12.1 ± 6.7	5.2–27.8
$VLDL_1$ TG production (mg/day/kg bw)			218 ± 76	107–347
$VLDL_1$-to-$VLDL_2$ TG transfer (mg/day/kg bw)			61.2 ± 36.8	20.9–146
$VLDL_2$ TG direct production (mg/day/kg bw)			27.2 ± 11.6	9.5–52
VLDL TG production (mg/day/kg bw)			245 ± 79	138–387
$VLDL_1$ apoB FCR (pools/day)			12.7 ± 7.5	4.31–31.0
$VLDL_1$ apoB FDCR (pools/day)			5.32 ± 6.28	0–23
$VLDL_1$ apoB FTR (pools/day)			7.34 ± 3.44	2.08–13.5
$VLDL_2$ apoB FCR (pools/day)			5.95 ± 2.74	2.12–12.3
VLDL apoB FCR (pools/day)			5.64 ± 2.93	2.21–11.2
$VLDL_1$ apoB production (mg/day/kg bw)			6.9 ± 2.9	2.88–12.5
$VLDL_1$-to-$VLDL_2$ apoB transfer (mg/day/kg bw)			4.36 ± 2.44	1.79–10.0
$VLDL_2$ apoB direct production (mg/day/kg bw)			1.9 ± 0.6	1.0–3.0
VLDL apoB production (mg/day/kg bw)			8.9 ± 3.4	4.1–15.1

bw, body weight; FCR, fractional catabolic rate; FDCR, fractional direct catabolic rate; FTR, fractional transfer rate.

Tracer recycling

To understand the impact that intrahepatic glycerol recycling between compartments 14 and 21 has on the final VLDL TG kinetic parameters determined in the model, we undertook a sensitivity analysis in which $k(21,14)$ or $k(14,21)$ was varied by 100% from the optimal value and the model was allowed to fit the observed data. It was found that variation in these parameters across this range altered the final VLDL TG production by less than 20% (5.5 ± 5.9% and 5 ± 4.6% for $VLDL_1$ and $VLDL_2$ production, respectively) and VLDL clearance by less than 25% ($VLDL_1$ FCR, 5.4 ± 5.4%; $VLDL_1$ FDCR, 6.3 ± 6.8%; and $VLDL_2$ FCR, 6.8 ± 7.7%). The largest relative change was when $k(21,14)$ was decreased by 50%; with smaller changes, the relative difference was much less. Thus, the model is practically insensitive to hepatic fluxes of glycerol and TG.

Impact of deuterium atom loss for the determination of glycerol enrichment in TG

It is known that glycerol during metabolic interconversions in the liver can lose deuterium atoms. In theory, this will result in a reduced apparent enrichment (i.e., the m+2/m0 value will vary to some degree depending on the extent to which there has been loss of one deuterium from the fragment that has been detected as m+3). Therefore, we compared the enrichment curves generated by analysis of the m+3 and m+2 ion mass fragments and by the mass ratios of m+3 (148), m+2 (147), m+1 (146), and m0 (145) in three subjects (**Fig. 3**). The results showed that the atom percentage excess in $VLDL_1$ averaged for three subjects was similar when using a fixed m+2/m0 measured at baseline or when using m+2/m0 calculated at each time point (Fig. 3). This result shows that the theoretical reduced apparent enrichment made no difference to the kinetic modeling.

Correlations of plasma TG to calculated values

Total plasma TG did not correlate significantly with the production rates of TG or apoB in total VLDL or in its subclasses (data not shown). However, total plasma TG did show a negative relationship to $VLDL_1$ FCR in both apoB ($P = 0.001$) and TG ($P < 0.01$) and to $VLDL_2$ FCR (apoB, $P < 0.01$; TG, $P < 0.05$).

Correlations of $VLDL_1$ and $VLDL_2$ concentrations

Analysis showed significant correlation between $VLDL_1$ apoB concentration and $VLDL_1$ apoB production ($P < 0.05$) and a significant negative correlation between $VLDL_1$ apoB concentration and $VLDL_1$ apoB FCR ($P < 0.001$) (**Fig. 4**). The $VLDL_2$ apoB concentration did correlate to $VLDL_2$ apoB direct production ($P < 0.05$) and correlated to transfer from $VLDL_1$ ($P < 0.01$) and it showed a negative correlation to $VLDL_2$ FCR ($P < 0.05$). The $VLDL_1$ TG concentration showed a positive correlation to $VLDL_1$ TG production ($P < 0.05$) and a negative correlation to $VLDL_1$ TG FCR ($P < 0.001$) (Fig. 4). Removal of TG from $VLDL_1$ includes the FTR and the FDCR, and the FDCR showed a significant inverse correlation with the $VLDL_1$ TG concentration ($P < 0.001$). The FDCR for $VLDL_1$ TG includes both direct removal of TG by catabolism and removal by hydrolysis.

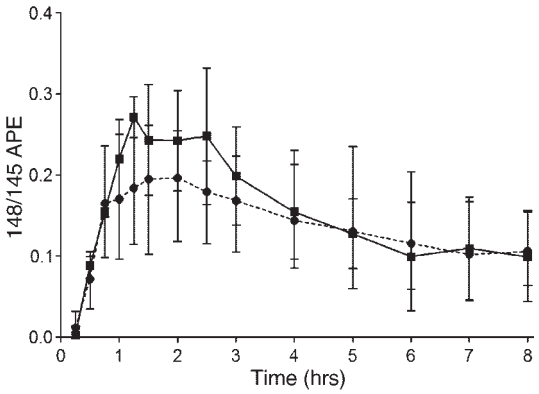

Fig. 3. $VLDL_1$ glycerol enrichment curve averaged for three subjects. To calculate isotope enrichments, the ratio between the ion mass fragments *m/z* 148 and *m/z* 147 (i.e., m+3/m+2) was multiplied with a fixed *m/z* 147:145 (i.e., m+2/m0) ratio measured at time point 0 (closed circles) or with a variable m+2/m0 measured at each time point (closed squares). The resulting *m/z* 148:145 values (i.e., m+3/m0) are expressed as atom percentage excess (APE). Errors bars indicate minimum and maximum values.

The $VLDL_2$ TG concentration did correlate with $VLDL_2$ TG direct production ($P < 0.05$) and with TG transferred from $VLDL_1$ ($P < 0.01$). There was a trend toward a negative correlation between the $VLDL_2$ TG pool and $VLDL_2$ TG FCR, but it was not significant (Fig. 4).

Analysis of the relation between TG and apoB concentrations in circulating $VLDL_1$ and $VLDL_2$ showed a highly significant correlation for both $VLDL_1$ and $VLDL_2$ (Fig. 4). Hence, the average TG/apoB ratio in $VLDL_1$ and $VLDL_2$ varied little between individuals (27.2 ± 3.6 in $VLDL_1$ and 6.1 ± 1.0 in $VLDL_2$) (Table 2).

Correlations of $VLDL_1$ and $VLDL_2$ production

The sizes of the secreted $VLDL_1$ and $VLDL_2$ particles from the liver can be estimated from the ratios of TG and apoB in the newly secreted lipoproteins. The newly secreted $VLDL_1$ particles were less variable in ratios (i.e., size) than newly secreted $VLDL_2$ particles (33.4 ± 8.4 vs. 14.3 ± 4.0) (Table 2). There was a strong correlation between $VLDL_1$ TG and $VLDL_1$ apoB production ($P < 0.005$). Likewise, there was a significant correlation for $VLDL_2$ direct apoB and TG production ($P < 0.005$) (Fig. 4). The analysis was performed using a linear correlation instead of a log-log correlation because the latter did not give a linear relation of the two quantities, despite almost the same coefficient (r) and significance (P).

Delay times

VLDL assembly has been proposed to occur in at least two steps, and it is envisaged that a precursor particle containing apoB-100 and a small complement of lipid coalesces with a large, apoB-free lipid droplet to form a TG-rich particle (12, 13, 32). However, support for this concept is based on in vitro data only. Therefore, we analyzed the delay times for apoB and TG. The [$^2H_5$]glycerol was rapidly incorporated into triacylglycerol and entered the blood system as VLDL TG after 21 ± 3.6 min (mean ± SD). In contrast, apoB-100 labeled with [$^2H_3$]leucine did not appear in the circulation as VLDL apoB until after 33 ± 6 min. Thus, the difference was 12 ± 5.4 min.

DISCUSSION

In this study, we developed a tracer model for apoB-100 and TG kinetics in VLDL subclasses and tested it in 17 subjects with lipid values representative of a Western population. We chose to model apoB and TG kinetics simultaneously in an arrangement in which all apoB compartments have corresponding TG compartments and to couple these at certain points in the model. This strategy made it possible to model both the apoB and TG $VLDL_1$ and $VLDL_2$ kinetics and to follow both direct catabolism and transfer of the lipoprotein particles. Before arriving at the current model, we tested several different approaches and alterations. For example, we found it necessary to include two compartments for the hydrolysis chain in both the $VLDL_1$ and $VLDL_2$ submodels. Chains with three or more compartments yielded no improvement, and a single compartment did not fit the data. We also found that it was not necessary to allow the lipoprotein particles to enter the hydrolysis chain in compartments 6 and 10, because this resulted in zero flux into these compartments. In designing the model, we decided to have compartments with particles of uniform size (i.e., uniform TG/apoB ratio) only, because the mass of TG being transferred corresponds to the size of the particles times the number of particles. This limits the model to four distinct particle sizes, apart from the particles in compartments 7 and 9. However, including more compartments, and therefore more possible sizes, did not improve the fit.

We also compared our results with earlier studies. In a recent comprehensive review, Marsh et al. (33) summarized the VLDL FCRs from 29 studies, the VLDL production from 27 studies, and the $VLDL_1$ and $VLDL_2$ FCRs and production values from eight studies. The total VLDL, $VLDL_1$ and $VLDL_2$ production, and catabolic rates of the calculated apoB values corresponded well with the values calculated with our multicompartment model. Furthermore, the total TG production corresponded well with the 5–46 g/day for total VLDL TG calculated by Carpentier et al. (15) using a monoexponential model. The total VLDL TG FCR varied from 0.22 to 1.2 pools/h, which also corresponded well with the results reported by Carpentier et al. (15). Thus, estimated values extracted from the model compared well with calculated values and results from earlier studies.

Several important findings were gained with the model. Analysis of the correlations showed that plasma TG was determined by the $VLDL_1$ and $VLDL_2$ apoB and TG FCRs. In fact, both the $VLDL_1$ and $VLDL_2$ concentrations are likely determined by their respective FCRs in these subjects. Looking at the actual curves for the relationship between the $VLDL_1$ and $VLDL_2$ apoB and TG concentrations and their respective FCRs reveals a curve-linear relationship. When omitting the two subjects with the highest apoB and TG pools, only the FCRs were significantly correlated

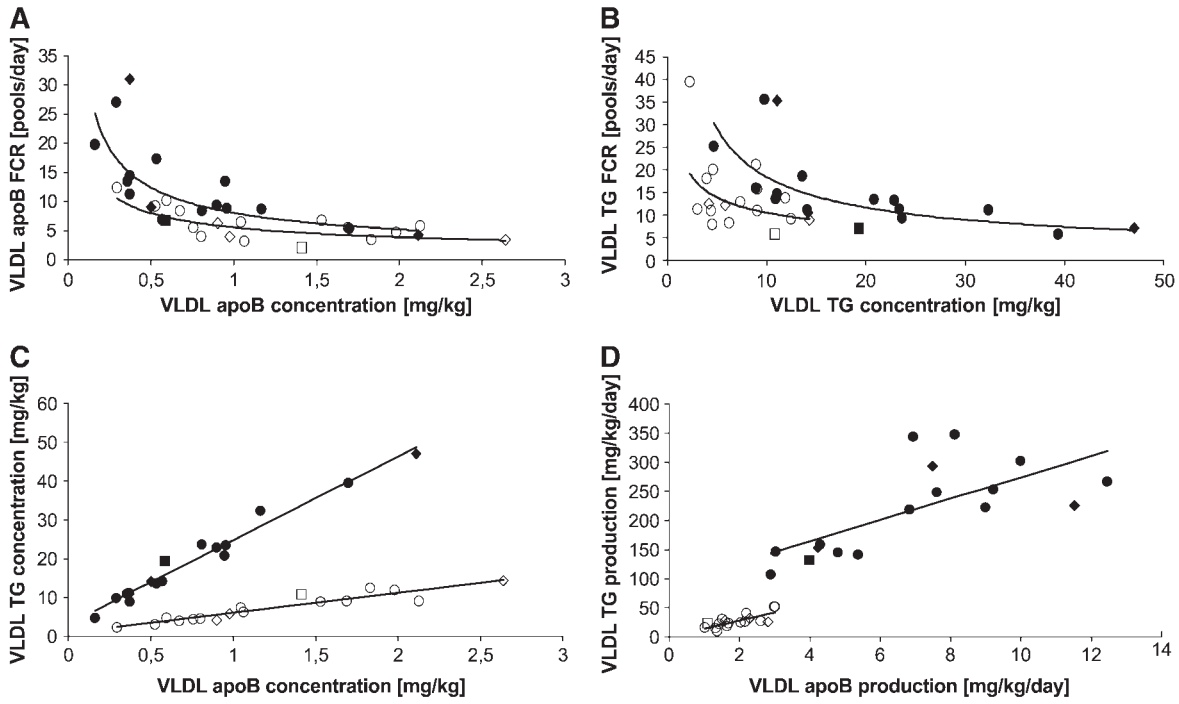

Fig. 4. Analysis of apoB or TG concentration versus mean residence time and TG/apoB ratios. Plots of measured apoB (top left) or TG (top right) concentration (mg/kg body weight) versus fractional catabolic rate (FCR; days), measured apoB concentration versus TG concentration (mg/kg body weight; bottom left), and apoB production versus TG production (mg/day/kg body weight; bottom right). The analysis of $VLDL_1$ (closed circles) and $VLDL_2$ (open circles) was performed on 17 subjects. One of these had a higher cholesterol value (7.5 mmol/l) than the remaining subjects: $VLDL_1$, closed squares; $VLDL_2$, open squares. Three subjects had higher body mass index (between 29.5 and 30.1 kg/m^2) than the remaining subjects: $VLDL_1$, closed diamonds; $VLDL_2$, open diamonds. The correlation between apoB concentration and apoB FCR in $VLDL_1$ ($P < 0.001$) and $VLDL_2$ ($P < 0.05$) is also shown. $VLDL_1$ TG concentration did correlate with $VLDL_1$ TG FCR ($P < 0.001$). The relation between TG and apoB concentrations in circulating $VLDL_1$ and $VLDL_2$ showed a highly significant correlation for both $VLDL_1$ and $VLDL_2$, ($P < 0.001$ and $P < 0.001$, respectively). There was a strong correlation between $VLDL_1$ TG and $VLDL_1$ apoB production ($P < 0.005$) and a correlation between $VLDL_2$ TG and $VLDL_2$ apoB production ($P < 0.005$).

to the pool sizes. This indicates that in healthy subjects with low pool sizes, the fasting concentrations are determined by the lipolysis rather than the production rate. However, extending the range of plasma TG and VLDL apoB and TG pool sizes might reveal a correlation to production rates. This finding is in agreement with studies by Packard et al. (26), who originally showed this for apoB $VLDL_1$.

The model showed a linear correlation between the $VLDL_1$ TG and apoB production. Furthermore, the composition of the $VLDL_1$ and $VLDL_2$ particles (TG/apoB ratio) in plasma suggests that a high level of total plasma TG is achieved mainly by an increased $VLDL_1$ TG pool, but this is the effect of an increased number of particles rather than increased particle size. Overall, the contributions of $VLDL_2$ TG pools to the total plasma TG levels were less than that of the $VLDL_1$ TG pools. We speculate that the $VLDL_2$ secretion reflects baseline production of TG, whereas the $VLDL_1$ secretion is modulated by dynamic variations in substrate fluxes. This is consistent with studies showing that insulin does not affect the direct production of $VLDL_2$ apoB or the lipid composition of the $VLDL_2$ particles (9).

The model also revealed a significant difference in the delay times of glycerol and leucine (i.e., VLDL TG and VLDL apoB). After incorporation of glycerol into TG, the completed lipoprotein enters the blood system within 21 min. In contrast, the delay time for apoB molecules is 33 min. These observations are consistent with a sequential assembly model of VLDL and likely provide the first evidence in humans that TG can be added to a primordial apoB-containing particle in the liver (12, 32). The data did not show a difference in delay time between $VLDL_1$ and $VLDL_2$. However, such studies need more frequent early sampling times than were used in this study.

In vivo, $VLDL_2$ particles are generated by direct synthesis in the liver or by intravascular lipolysis of $VLDL_1$ particles (10, 26). In our model, however, $VLDL_2$ particles had the same kinetics regardless of their origin. This is a tentative caveat, because differences in the apolipoprotein or lipid composition of $VLDL_2$ particles from these two sources could affect their kinetics. However, we avoided separating the pathways for these lipoproteins in the model because this simplification did not cause any problem during the modeling and because separation of the pathways would have complicated the model.

Since the planning of these studies, improved techniques have been developed for assessing the d5-glycerol tracer as an entire moiety in GC-MS analysis (3, 8). The derivation of VLDL TG kinetics using the GC-MS method used in this study could theoretically lead to the potential loss of deuterium from d5-glycerol tracer during the meta-

bolic process in the liver. However, we found experimentally that this did not invalidate the approach we adopted, but it is possible that higher TG turnover rates would have been obtained with the technique developed by Patterson and coworkers (3, 8). For the glycerol model, we used population means. We compared the results using population means and the actual plasma glycerol curves in three subjects with plasma TG in the range of 1.23–2.77 mmol/l. The derived results (i.e., production and catabolic rates) were similar in the two models. However, if subjects with severe dyslipidemia are analyzed, the population means for these subjects must be verified or the plasma glycerol enrichments must be used. The current data do not allow us to verify the actual hepatic TG model. New experiments and emerging knowledge, including the quantification of liver fat in humans, may allow this in future studies.

In summary, we developed and tested a multicompartment model that allows the kinetic parameters of TG and apoB-100 in $VLDL_1$ and $VLDL_2$ to be simultaneously determined after a bolus of [$^2H_3$]leucine and [$^2H_5$]glycerol. We suspect that the model will be useful for understanding how the lipid metabolism is disrupted in patients with dyslipidemias.

APPENDIX

Q_i denotes the tracee mass in compartment i. The $VLDL_1$ apoB compartments are 5, 6, and 7 and the corresponding $VLDL_1$ TG compartments are 15, 16, and 17. The $VLDL_2$ apoB compartments are 8, 9, and 10 and the corresponding $VLDL_2$ TG compartments are 18, 19, and 20. l_{apoB} is the total amount of apoB synthesized in the liver, and l_{TG} is the total amount of TG synthesized in the liver. The fraction of apoB going to $VLDL_1$ is denoted d_5, and the fraction going to $VLDL_2$ is denoted d_8 ($= 1 - d_5$). Analogously, the corresponding fractions for TG are denoted d_{15} and d_{18}. We get the following equations for compartments 5 and 6:

$$\frac{dQ_5}{dt} = d_5 L_{apoB} - (k_{6,5} + k_{7,5}) Q_5 \qquad (A1)$$

$$\frac{dQ_6}{dt} = k_{6,5} Q_5 - (k_{8,6} + k_{0,6}) Q_6 \qquad (A2)$$

Equations A1 and A2 describe the apoB kinetics. Multiplying Eq. A1 by A_5 and Eq. A2 by A_6, assuming steady state, we have A_5 and A_6 constant, and

$$\frac{dQ_{15}}{dt} = d_5 A_5 L_{apoB} - (k_{6,5} + k_{7,5}) Q_{15} \qquad (A3)$$

$$\frac{dQ_{16}}{dt} = k_{6,5}\frac{A_6}{A_5} Q_{15} - (k_{8,6} + k_{0,6}) Q_{16} \qquad (A4)$$

where we have used $A_5 Q_5 = Q_{15}$ and $A_6 Q_6 = Q_{16}$. Defining A_5 to be the ratio of the fluxes of TG and apoB going into compartment 5, $A_5 = (d_{15} l_{TG}) / (d_5 l_{apoB})$. Furthermore, letting $A_6 = A_5 f_{6,5}$, etc., and rewriting the equations we get the following:

$$\frac{dQ_{15}}{dt} = d_{15} L_{TG} - (f_{6,5} k_{6,5} + f_{7,5} k_{7,5} + (1 - f_{6,5}) k_{6,5} + (1 - f_{7,5}) k_{7,5}) Q_{15} \qquad (A3a)$$

$$\frac{dQ_{16}}{dt} = k_{6,5} f_{6,5} Q_{15} - ((1 - f_{8,6}) k_{8,6} + f_{8,6} k_{8,6} + k_{0,6}) Q_{16} \qquad (A4a)$$

Let $k_{16,15} = k_{6,5} f_{6,5}$, $k_{0,15} = (1 - f_{6,5}) k_{6,5} + (1 - f_{7,5}) k_{7,5}$, $k_{17,15} = k_{7,5} f_{7,5}$, $k_{0,17} = k_{0,7}$, $k_{18,16} = k_{8,6} f_{8,6}$, $k_{0,16} = (1 - f_{8,6}) k_{8,6} + k_{0,6}$.

$$\frac{dQ_{15}}{dt} = d_{15} L_{TG} - (k_{16,15} + k_{0,15}) Q_{15} \qquad (A3b)$$

$$\frac{dQ_{16}}{dt} = k_{16,15} Q_{16} - (k_{18,16} + k_{0,16}) Q_{16} \qquad (A4b)$$

When a particle is transferred from a compartment to another compartment, only a fraction of the TG reaches the destination compartment. The rest is removed by hydrolysis. However, the source compartment detects a loss of the whole particle. Here, $f_{6,5}$ denotes the fraction of the TG that is kept during the transfer. The general definition for the fractional transfer coefficients in the TG model is as follows:

$$k_{j+10,\,i+10} = f_{j,i} k_{j,i}, \quad k_{0,i+10} = k_{0,i} + \sum_{j=5}^{10} (1 - f_{j,i}) k_{j,i}$$

where $i, j, = 5, \ldots 10$. These definitions of fractional transfer coefficients give a system of equations for the transport of TG that is similar to the transport of apoB. Both systems of equations fulfill the requirements for compartmental systems. The parameters to determine in the model are the $f_{j,i}$ values.

The data available do not allow for the separation of pathways for $VLDL_2$ secreted directly from the liver and $VLDL_2$ produced from $VLDL_1$ particles as described (25). Therefore, we constrain the model by defining newly secreted $VLDL_2$ particles and particles transferred from $VLDL_1$ (from compartment 6 to compartment 8) to have the same TG/apoB ratio (A_8). Thus, the fraction of TG secreted into $VLDL_1$ and $VLDL_2$ is as follows:

$$A_8 = \frac{(1 - d_{15}) L_{TG}}{(1 - d_5) L_{apoB}} = f_{8,6} f_{6,5} A_5 = f_{8,6} f_{6,5} \frac{d_{15} L_{TG}}{d_5 L_{apoB}}$$

Or

$$d_{15} = \frac{d_5}{d_5 + f_{8,6} f_{6,5} (1 - d_5)}.$$

The authors thank Dr. Olle Nerman for constructive discussions, Hannele Hilden, Helinä Perttunen-Nio, and Dorothy Bedford for expert technical assistance, and Stephen Ordway for editing of the manuscript. This work was supported by the Swedish Research Council, the Swedish Foundation for Strategic Research, the Söderberg Foundation, the Sigrid Juselius Foundation, the Helsinki University Central Hospital Research Foundation, and the Stochastic Center at Chalmers University of Technology, Göteborg, Sweden.

REFERENCES

1. Cryer, D. R., T. Matsushima, J. B. Marsh, M. Yudkoff, P. M. Coates, and J. A. Cortner. 1986. Direct measurement of apolipoprotein B synthesis in human very low density lipoprotein using stable isotopes and mass spectrometry. *J. Lipid Res.* **27:** 508–516.
2. Cohn, J. S., D. A. Wagner, S. D. Cohn, J. S. Millar, and E. J. Schaefer. 1990. Measurement of very low density and low density lipoprotein apolipoprotein (apo) B-100 and high density lipopro-

tein apo A-I production in human subjects using deuterated leucine. Effect of fasting and feeding. *J. Clin. Invest.* **85:** 804–811.
3. Patterson, B. W., B. Mittendorfer, N. Elias, R. Satyanarayana, and S. Klein. 2002. Use of stable isotopically labeled tracers to measure very low density lipoprotein-triglyceride turnover. *J. Lipid Res.* **43:** 223–233.
4. Zech, L. A., S. M. Grundy, D. Steinberg, and M. Berman. 1979. Kinetic model for production and metabolism of very low density lipoprotein triglycerides. Evidence for a slow production pathway and results for normolipidemic subjects. *J. Clin. Invest.* **63:** 1262–1273.
5. Melish, J., N. A. Le, H. Ginsberg, D. Steinberg, and W. V. Brown. 1980. Dissociation of apoprotein B and triglyceride production in very-low-density lipoproteins. *Am. J. Physiol.* **239:** E354–E362.
6. Harris, W. S., W. E. Connor, D. R. Illingworth, D. W. Rothrock, and D. M. Foster. 1990. Effects of fish oil on VLDL triglyceride kinetics in humans. *J. Lipid Res.* **31:** 1549–1558.
7. Barrett, P. H., N. Baker, and P. J. Nestel. 1991. Model development to describe the heterogeneous kinetics of apolipoprotein B and triglyceride in hypertriglyceridemic subjects. *J. Lipid Res.* **32:** 743–762.
8. Patterson, B. W. 2002. Methods for measuring lipid metabolism in vivo. *Curr. Opin. Clin. Nutr. Metab. Care.* **5:** 475–479.
9. Malmstrom, R., C. J. Packard, M. Caslake, D. Bedford, P. Stewart, H. Yki-Jarvinen, J. Shepherd, and M. R. Taskinen. 1997. Defective regulation of triglyceride metabolism by insulin in the liver in NIDDM. *Diabetologia.* **40:** 454–462.
10. Malmstrom, R., C. J. Packard, T. D. Watson, S. Rannikko, M. Caslake, D. Bedford, P. Stewart, H. Yki-Jarvinen, J. Shepherd, and M. R. Taskinen. 1997. Metabolic basis of hypotriglyceridemic effects of insulin in normal men. *Arterioscler. Thromb. Vasc. Biol.* **17:** 1454–1464.
11. Packard, C. J., and J. Shepherd. 1997. Lipoprotein heterogeneity and apolipoprotein B metabolism. *Arterioscler. Thromb. Vasc. Biol.* **17:** 3542–3556.
12. Boren, J., S. Rustaeus, and S. O. Olofsson. 1994. Studies on the assembly of apolipoprotein B-100- and B-48-containing very low density lipoproteins in McA-RH7777 cells. *J. Biol. Chem.* **269:** 25879–25888.
13. Olofsson, S. O., L. Asp, and J. Boren. 1999. The assembly and secretion of apolipoprotein B-containing lipoproteins. *Curr. Opin. Lipidol.* **10:** 341–346.
14. Lemieux, S., B. W. Patterson, A. Carpentier, G. F. Lewis, and G. Steiner. 1999. A stable isotope method using a [(2)H(5)]glycerol bolus to measure very low density lipoprotein triglyceride kinetics in humans. *J. Lipid Res.* **40:** 2111–2117.
15. Carpentier, A., B. W. Patterson, N. Leung, and G. F. Lewis. 2002. Sensitivity to acute insulin-mediated suppression of plasma free fatty acids is not a determinant of fasting VLDL triglyceride secretion in healthy humans. *Diabetes.* **51:** 1867–1875.
16. Lindgren, F. T., L. C. Jensen, and F. T. Hatch. 1972. The isolation and quantitative analysis of serum lipoproteins. *In* Blood Lipids and Lipoproteins: Quantitation, Composition, and Metabolism. G. J. Nelson, editor. John Wiley & Sons, New York. 181–274.
17. Mero, N., M. Syvanne, B. Eliasson, U. Smith, and M. R. Taskinen. 1997. Postprandial elevation of apoB-48-containing triglyceride-rich particles and retinyl esters in normolipemic males who smoke. *Arterioscler. Thromb. Vasc. Biol.* **17:** 2096–2102.
18. Vakkilainen, J., K. V. Porkka, I. Nuotio, P. Pajukanta, L. Suurinkeroinen, K. Ylitalo, J. S. Viikari, C. Ehnholm, and M. R. Taskinen. 1998. Glucose intolerance in familial combined hyperlipidaemia. EUFAM Study Group. *Eur. J. Clin. Invest.* **28:** 24–32.
19. Kashyap, M. L., B. A. Hynd, and K. Robinson. 1980. A rapid and simple method for measurement of total protein in very low density lipoproteins by the Lowry assay. *J. Lipid Res.* **21:** 491–495.
20. Egusa, G., D. W. Brady, S. M. Grundy, and B. V. Howard. 1983. Isopropanol precipitation method for the determination of apolipoprotein B specific activity and plasma concentrations during metabolic studies of very low density lipoprotein and low density lipoprotein apolipoprotein B. *J. Lipid Res.* **24:** 1261–1267.
21. Demant, T., C. J. Packard, H. Demmelmair, P. Stewart, A. Bedynek, D. Bedford, D. Seidel, and J. Shepherd. 1996. Sensitive methods to study human apolipoprotein B metabolism using stable isotope-labeled amino acids. *Am. J. Physiol.* **270:** E1022–E1036.
22. Witter, R. F., and V. S. Whitner. 1972. Determination of serum triglycerides. *In* Blood Lipids and Lipoproteins: Quantification, Composition, and Metabolism. G. J. Nelson, editor. John Wiley & Sons, New York. 75–105.
23. Patterson, B. W., G. Zhao, N. Elias, D. L. Hachey, and S. Klein. 1999. Validation of a new procedure to determine plasma fatty acid concentration and isotopic enrichment. *J. Lipid Res.* **40:** 2118–2124.
24. Beylot, M., C. Martin, B. Beaufrere, J. Riou, and R. Mornex. 1987. Determination of steady state and nonsteady-state glycerol kinetics in humans using deuterium-labeled tracer. *J. Lipid Res.* **28:** 414–422.
25. Packard, C. J., A. Gaw, T. Demant, and J. Shepherd. 1995. Development and application of a multicompartmental model to study very low density lipoprotein subfraction metabolism. *J. Lipid Res.* **36:** 172–187.
26. Packard, C. J., T. Demant, J. P. Stewart, D. Bedford, M. J. Caslake, G. Schwertfeger, A. Bedynek, J. Shepherd, and D. Seidel. 2000. Apolipoprotein B metabolism and the distribution of VLDL and LDL subfractions. *J. Lipid Res.* **41:** 305–318.
27. Griffin, B. A., and C. J. Packard. 1994. Metabolism of VLDL and LDL subclasses. *Curr. Opin. Lipidol.* **5:** 200–206.
28. Malmstrom, R., C. J. Packard, M. Caslake, D. Bedford, P. Stewart, J. Shepherd, and M. R. Taskinen. 1999. Effect of heparin-stimulated plasma lipolytic activity on VLDL APO B subclass metabolism in normal subjects. *Atherosclerosis.* **146:** 381–390.
29. Malmstrom, R., C. J. Packard, M. Caslake, D. Bedford, P. Stewart, H. Yki-Jarvinen, J. Shepherd, and M. R. Taskinen. 1998. Effects of insulin and acipimox on VLDL1 and VLDL2 apolipoprotein B production in normal subjects. *Diabetes.* **47:** 779–787. [Erratum. 1998. *Diabetes.* **47:** 1532.]
30. Zech, L. A., R. C. Boston, and D. M. Foster. 1986. The methodology of compartmental modeling as applied to the investigation of lipoprotein metabolism. *Methods Enzymol.* **129:** 366–384.
31. Adiels, M. 2002. A Compartmental Model for Kinetics of Apolipoprotein B-100 and Triglycerides in $VLDL_1$ and $VLDL_2$ in Normolipidemic Subjects. Licentiate Thesis. Chalmers University of Technology, Göteborg, Sweden.
32. Alexander, C. A., R. L. Hamilton, and R. J. Havel. 1976. Subcellular localization of B apoprotein of plasma lipoproteins in rat liver. *J. Cell Biol.* **69:** 241–263.
33. Marsh, J. B., F. K. Welty, A. H. Lichtenstein, S. Lamon-Fava, and E. J. Schaefer. 2002. Apolipoprotein B metabolism in humans: studies with stable isotope-labeled amino acid precursors. *Atherosclerosis.* **162:** 227–244.